



<b>Title</b>	<b>Depth profiling of Si nanocrystals in Si-implanted SiO<sub>2</sub> films by spectroscopic ellipsometry</b>
<b>Author(s)</b>	<b>Chen, TP; Liu, Y; Tse, MS; Ho, PF; Dong, G; Fung, S</b>
<b>Citation</b>	<b>Applied Physics Letters, 2003, v. 81 n. 25, p. 4724-4726</b>
<b>Issued Date</b>	<b>2003</b>
<b>URL</b>	<b><a href="http://hdl.handle.net/10722/42475">http://hdl.handle.net/10722/42475</a></b>
<b>Rights</b>	<b>Creative Commons: Attribution 3.0 Hong Kong License</b>

# Depth profiling of Si nanocrystals in Si-implanted SiO<sub>2</sub> films by spectroscopic ellipsometry

T. P. Chen,<sup>a)</sup> Y. Liu, M. S. Tse, and P. F. Ho

*School of Electrical and Electronic Engineering, Nanyang Technological University, Singapore 639798*

Gui Dong

*Institute of Microelectronics, Singapore Science Park II, Singapore 117685*

S. Fung

*Department of Physics, The University of Hong Kong, Pokfulam Road, Hong Kong*

(Received 30 April 2002; accepted 16 October 2002)

In this letter, we report an approach to depth profiling of Si nanocrystals embedded in SiO<sub>2</sub> film based on spectroscopic ellipsometry. The SiO<sub>2</sub> film is divided into many sublayers with equal thickness, and each sublayer is characterized by its nanocrystal concentration. In the spectral fittings, the effective dielectric function of each sublayer is obtained from an effective medium approximation by using the dielectric function of Si nanocrystal that is calculated with either the bond contraction or the phenomenological models for the band gap expansion of nanocrystals. The fittings yield the nanocrystal depth profiles and the nanocrystal sizes as well. The depth profiles from the two models are similar, and they are in good agreement with secondary ion mass spectroscopy analysis. © 2002 American Institute of Physics. [DOI: 10.1063/1.1528286]

SiO<sub>2</sub> films containing Si nanocrystals have recently attracted much attention because of their light-emitting ability that can be used for Si-based optoelectronic applications.<sup>1</sup> In addition, they have also regained interest as possible candidates for the application of single electron memory devices or other single-electron devices.<sup>2–5</sup> One of the promising techniques being used to elaborate nanocrystals is the implantation of Si ions into SiO<sub>2</sub> films that are thermally grown on Si substrates.<sup>6–8</sup> The SiO<sub>2</sub> has proven to be a robust matrix that provides good chemical and electrical passivation of the nanocrystals. In addition, the fabrication is fully compatible with the mainstream complementary metal–oxide–semiconductor processes, allowing the integration of the optoelectronic devices into the Si circuits. Therefore, this technique is very attractive. For applications it is essential to have detailed information on the depth distributions of the nanocrystals in the SiO<sub>2</sub> films. In this letter, we report a cheap and nondestructive approach, based on spectroscopic ellipsometry, to determine the depth profiles of nanocrystals in Si-implanted SiO<sub>2</sub> films.

SiO<sub>2</sub> films 550 nm thick were grown on *p*-type Si (100) substrates by wet oxidation of Si at 1000 °C. The SiO<sub>2</sub> films were implanted with a dose of  $1 \times 10^{17}$  atoms/cm<sup>2</sup> of Si<sup>+</sup> at 50 keV. Afterwards, the samples were annealed at 1000 °C for duration of 1 h. Upon such an annealing, one would expect the formation of Si nanocrystals in the SiO<sub>2</sub> film.<sup>8,9</sup> As revealed by the spectroscopic ellipsometry analysis and secondary ion mass spectroscopy (SIMS) measurements discussed later, the nanocrystals distribute from the surface to a depth of about 250 nm.

As the concentration of the nanocrystals in the SiO<sub>2</sub> film varies with the depth, the optical properties of the film will vary with the depth also. To reflect the variation of the nanocrystal concentration with the depth, the film is divided into

*m* sublayers with equal thickness  $d = T_{\text{ox}}/m$ , where  $T_{\text{ox}}$  is the total thickness of the film, that is, sublayers 1, 2, ..., *m* from the surface to the SiO<sub>2</sub>/Si interface ( $m = 22$  in this study), and the nanocrystal concentration is considered constant within each sublayer. Each sublayer has its own complex refractive index,  $N_i = n_i + jk_i$  ( $i = 1, 2, \dots, m$ ) where  $n_i$  and  $k_i$  are the refractive index and extinction coefficient for the *i*th sublayer, respectively. Note that  $N_i$  is also a function of wavelength ( $\lambda$ ). Therefore, one can use a ( $m + 2$ )-phase model, that is, air/sublayer 1/.../sublayer *m*/Si substrate, for the ellipsometry analysis. Each phase is characterized by its complex refractive index,  $N_i$  ( $i = 0, 1, \dots, m, m + 1$ ). Note that  $N_0 = 1$  for air and  $N_{m+1} = N_{\text{Si}}$  (i.e., the Si complex refractive index) for the Si substrate. For a fixed incident angle  $\phi_0$  and a given  $d$  ( $\phi_0 = 75^\circ$  and  $d = 25$  nm in this study), the ellipsometric angles  $\psi$  and  $\Delta$  are functions of the parameters  $N_1, N_2, \dots, N_m, N_{\text{Si}}$  and  $\lambda$ .<sup>10,11</sup>

For each sublayer, its effective complex dielectric function  $\epsilon_i$  ( $= N_i^2, i = 1, 2, \dots, m$ ) can be calculated with the following effective medium approximation<sup>10,12</sup>

$$\frac{\epsilon_i - \epsilon_{\text{SiO}_2}}{\epsilon_i + 2\epsilon_{\text{SiO}_2}} = \nu_i \frac{\epsilon_{\text{nc-Si}} - \epsilon_{\text{SiO}_2}}{\epsilon_{\text{nc-Si}} + 2\epsilon_{\text{SiO}_2}}, \quad (1)$$

where  $\nu_i$  ( $i = 1, 2, \dots, m$ ) is the volume fraction (it will be converted to atom percentage later) of the nanocrystals in the *i*th sublayer,  $\epsilon_{\text{SiO}_2}$  is the dielectric function of host material SiO<sub>2</sub>, and  $\epsilon_{\text{nc-Si}}$  is the dielectric function of Si nanocrystal. Using Eq. (1), the depth distribution of the complex refractive index is converted to the depth distribution of the volume fraction ( $\nu_i$ ). Thus,  $\psi$  and  $\Delta$  can be symbolically written as

$$\Psi = f_1(\nu_1, \nu_2, \dots, \nu_m, N_{\text{nc-Si}}, N_{\text{SiO}_2}, N_{\text{Si}}, \lambda) \quad (2)$$

and

$$\Delta = f_2(\nu_1, \nu_2, \dots, \nu_m, N_{\text{nc-Si}}, N_{\text{SiO}_2}, N_{\text{Si}}, \lambda). \quad (3)$$

<sup>a)</sup>Electronic mail: echentp@ntu.edu.sg

The functions  $f_1$  and  $f_2$  cannot be expressed as analytical formulas, but  $\psi$  and  $\Delta$  can be calculated numerically with the functions. As the complex refractive indexes of  $\text{SiO}_2$  and Si (i.e.,  $N_{\text{SiO}_2}$  and  $N_{\text{Si}}$ ) are well known, if the complex refractive index of Si nanocrystal is also known, the depth profile of the nanocrystal concentration can be found by searching for one set of  $(\nu_1, \nu_2, \dots, \nu_m)$  such that the following error function:

$$F = \sum_{\lambda} [(\Psi_m^{\lambda} - \Psi_c^{\lambda})^2 + (\Delta_m^{\lambda} - \Delta_c^{\lambda})^2] \quad (4)$$

is a minimum for the whole measured spectral range, where  $\Psi_m^{\lambda}$  and  $\Delta_m^{\lambda}$  are the respective measured  $\Psi$  and  $\Delta$  values at  $\lambda$ , and  $\Psi_c^{\lambda}$  and  $\Delta_c^{\lambda}$  are the calculated  $\Psi$  and  $\Delta$  values with Eqs. (2) and (3), respectively, at the same wavelength. Actually, this is a spectral fitting over a wide range of wavelengths. In this study, this spectral fitting was carried out in the wavelength range of 400 to 1200 nm. This fitting procedure has been proven correct and effective by its successful application to the well-known system of pure  $\text{SiO}_2$  film on Si substrate.

To apply the fitting procedure to  $\text{SiO}_2$  films containing Si nanocrystals, we must know the dielectric function of Si nanocrystal. It is questionable to use the dielectric function of bulk crystalline Si for the nanocrystal, as it is expected that with size reduction of a nanometric system, its dielectric function will change. Nevertheless, as a trial, we used the dielectric function of bulk crystalline Si in the fitting, and the best fitting is shown in Fig. 1(a). As can be seen in Fig. 1(a), although the agreement between the measurement and the calculation is not too good, all the complicated spectral features of the experimental  $\Psi$  and  $\Delta$  are basically fitted by the calculation. This indicates that the difference of dielectric functions between bulk crystalline Si and Si nanocrystal is not huge, implying that the sizes of the nanocrystals are not too small (say, not less than 3 nm) in this study.

The dielectric function of Si nanocrystal can be calculated by using the simple formulas proposed in<sup>13</sup> which are duplicated in the following for easy reference. As a result of the band-gap expansion ( $\Delta E_g$ ) due to the reduction of nanocrystal size, the change ( $\Delta\chi$ ) of the dielectric susceptibility is given by

$$\Delta\chi/\chi_0 = -2(\Delta E_g/E_{g0}), \quad (5)$$

and the change ( $\Delta\epsilon_m$ ) of the imaginary part of the complex dielectric function is given as

$$\Delta\epsilon_m/\epsilon_{m0} = -2[E_{g0}/(E - E_{g0})](\Delta E_g/E_{g0}), \quad (6)$$

where  $\chi_0$ ,  $\epsilon_{m0}$ , and  $E_{g0}$  are the corresponding physical parameters of bulk crystalline Si, and  $E$  is photon energy. It should be pointed out that the formulas are just a first-order approximation valid for a small  $\Delta E_g/E_{g0}$ . To calculate the dielectric function of Si nanocrystal, the band-gap change  $\Delta E_g/E_{g0}$  should be known.

For comparison, here two different models are used to calculate the band-gap change. The first model is a phenomenological model, which predicts the trend for quantum confinement, that is, the inverse dependence of the expanded band gap on the nanocrystallite size, and in which a log-normal distribution of nanocrystallite sizes is considered.<sup>14</sup> From this model,  $\Delta E_g$  is given by

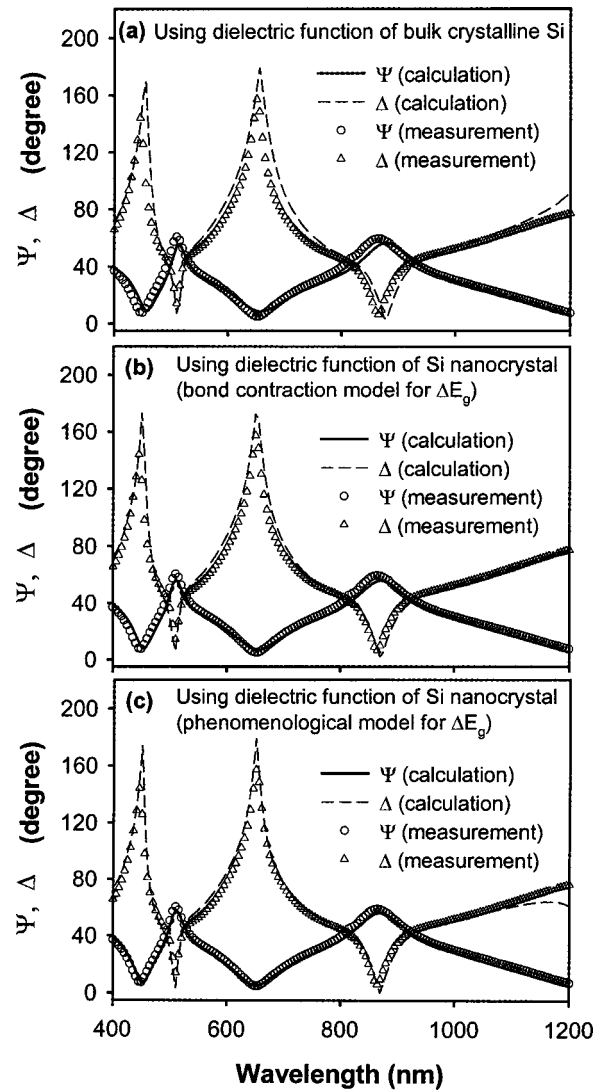


FIG. 1. Best spectral fittings of  $\Psi$  and  $\Delta$  with 161 wavelengths: (a) using the dielectric function of bulk crystalline Si; (b) using the dielectric function of Si nanocrystal calculated with the bond contraction model for  $\Delta E_g$ ; and (c) using the dielectric function of Si nanocrystal calculated with the phenomenological model for  $\Delta E_g$ . The values of  $F$  defined in Eq. (4) are 25679, 11331, and 8477 for the fittings shown in (a), (b), and (c), respectively.

$$\Delta E_g = \frac{C}{d_0^n} \left( \frac{d_m}{d_0} \right)^{n(2n+5)/3}, \quad (7)$$

where  $d_0$  (in nm) is the mean size of nanocrystals and  $d_m$  is the size for which the maximum occurs in the log-normal distribution,  $n = 1.22$ ,  $C = 3.9$ , and  $d_m/d_0 = 0.7$ .<sup>14</sup> The second model is the bond contraction model.<sup>13,15</sup> From this model, if the surface bond contraction is significant for only the two outermost atomic layers of a spherical dot and the dot size (i.e., the diameter  $D$ ) is much larger than the atomic diameter  $d$ , the band-gap expansion is given as

$$\frac{\Delta E_g}{E_{g0}} = \gamma'_1 c_1 (c_1^{-m} - 1) + \gamma'_2 c_2 (c_2^{-m} - 1), \quad (8)$$

where  $\gamma'_i = (3/k)[1 - (i - 0.5)/k]^2$  ( $i = 1, 2$ ),  $k = D/(2d)$ ,  $m = 1$ ,  $c_1 = 0.88$ , and  $c_2 = 0.94$ .<sup>13</sup> For a given nanocrystal size (i.e., the mean size  $d_0$  in the first model or the diameter  $D$  in the second model),  $\Delta E_g/E_{g0}$  can be calculated by using these two models, and thus the dielectric function of the Si nanocrystal can be obtained with Eqs. (5) and (6). Therefore,

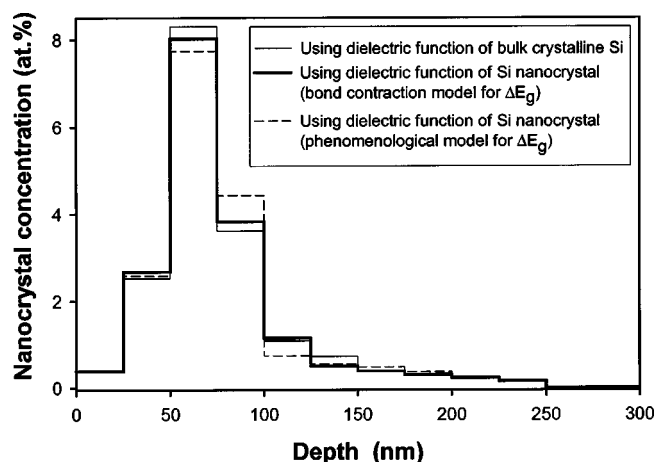


FIG. 2. Depth profiles of Si nanocrystals obtained from the spectral fittings by using the dielectric function of bulk crystalline Si or the dielectric function of Si nanocrystal calculated with either the bond contraction or phenomenological models for  $\Delta E_g$ .

the spectral fitting discussed previously is now carried out by searching for the nanocrystal size and one set of  $(\nu_1, \nu_2, \dots, \nu_m)$  such that the error function ( $F$ ) is a minimum.

Figures 1(b) and 1(c) show the best fittings with the band contraction model (the second model) and the phenomenological model (the first model) for  $\Delta E_g$ , respectively. As can be seen clearly in Fig. 1, these fittings, which have considered the nanosize effect on the band gap, are superior to the fitting with the dielectric function of bulk crystalline Si, indicating that the nanosize effect plays a role in the dielectric function. The depth profiles of Si nanocrystal concentration obtained from the fittings based on the two models are shown in Fig. 2, and they are also compared in this figure with the depth profile obtained from the fitting using the dielectric function of bulk crystalline Si. As can be seen in Fig. 2, the three depth profiles appear to be very similar (only some small difference exist in the peak regions of the profiles). The reason for this is that, as indicated by our calculations based on the two models, the difference of dielectric functions between the bulk crystalline Si and the Si nanocrystal is not large, as the size of the Si nanocrystals is not very small. The fitting based on the bond contraction model yields a nanocrystal size of about 5 nm, which agrees with the result reported in Ref. 8 for similar nanocrystal formation conditions, while the fitting based on the phenomenological model yields a size of about 9 nm. For such nanocrystal sizes, the bond contraction model (and the phenomenological model) gives a decrease of 9% (and 16%) in the real part and a decrease of 5% (and 9%) in the imaginary part of the dielectric function at the wavelength of 400 nm. Therefore, although the fittings can be improved by taking into account the small reductions in the dielectric function due to the size effect (as shown in Fig. 1), the reductions do not have a very significant impact on the depth profiles. The depth profiles agree with that from the SIMS measurement. Figure 3 shows the comparison of the depth profile obtained from the spectral fitting based on the bond contraction model with that from the secondary ion mass spectroscopy measurement. The good agreement indicates that the above approach for depth profiling is reliable.

In conclusion, we have developed an approach to deter-

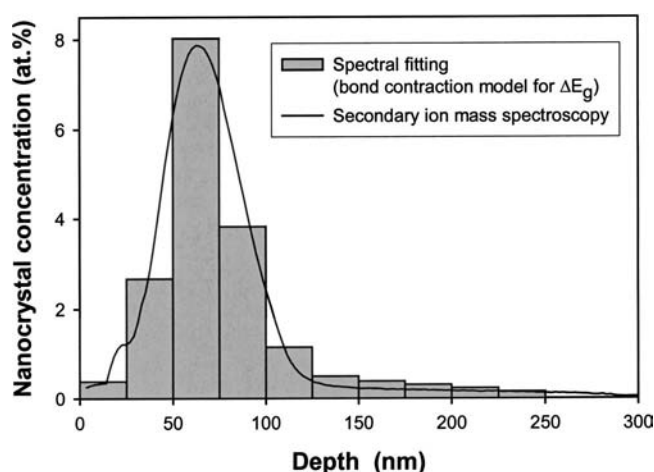


FIG. 3. Comparison of the result of SIMS with the depth profile obtained from the spectral fitting by using the dielectric function of Si nanocrystal calculated with the bond contraction model for  $\Delta E_g$ .

mine depth profiles of Si nanocrystals in  $\text{SiO}_2$  films based on spectroscopic ellipsometry. In the ellipsometry analysis, the  $\text{SiO}_2$  film with a depth distribution of Si nanocrystals is divided into  $m$  sublayers with equal thickness (a better depth resolution for a larger  $m$ ), and each sublayer is characterized by its nanocrystal concentration. As the dielectric function of  $\text{SiO}_2$  is well known, the effective dielectric function of each sublayer can be calculated with the effective medium approximation if the dielectric function of Si nanocrystal is also given. In the spectral fittings, the dielectric function of Si nanocrystal is calculated based on two different models (i.e., the bond contraction model and the phenomenological model) for the band-gap expansion due to the nanocrystal size reduction. The fittings yield the nanocrystal depth profile and the nanocrystal size as well. The depth profiles from the two models are very similar, and they are in good agreement with the SIMS measurement.

<sup>1</sup>L. Brus, in *Light Emission in Silicon: From Physics to Devices*, Semiconductors & Semimetals Vol. 49, edited by D. Lockwood (Academic, New York, 1998), pp. 303–328.

<sup>2</sup>S. Tiwari, F. Rana, H. Hanafi, A. Hartstein, E. F. Crabbé, and K. Chan, *Appl. Phys. Lett.* **68**, 1377 (1996).

<sup>3</sup>E. Kapetanakis, P. Normand, and D. Tsoukalas, *Appl. Phys. Lett.* **77**, 3450 (2000).

<sup>4</sup>E. A. Boer, M. L. Brongersma, and H. A. Atwater, *Appl. Phys. Lett.* **79**, 791 (2001).

<sup>5</sup>S.-H. Choi and R. G. Elliman, *Appl. Phys. Lett.* **75**, 968 (1999).

<sup>6</sup>M. L. Brongersma, A. Polman, K. S. Min, and H. A. Atwater, *J. Appl. Phys.* **86**, 759 (1999).

<sup>7</sup>S. Guha, *J. Appl. Phys.* **84**, 5210 (1998).

<sup>8</sup>B. Garrido, M. López, O. González, A. Pérez-Rodríguez, J. R. Morante, and C. Bonafos, *Appl. Phys. Lett.* **77**, 3143 (2000).

<sup>9</sup>S. Guha, S. B. Qadri, R. G. Musket, M. A. Wall, and T. Shimizu-Iwayama, *J. Appl. Phys.* **88**, 3954 (2000).

<sup>10</sup>E. A. Irene, in *In Situ Real-Time Characterization of Thin Films*, edited by O. Auciello and A. R. Krauss (Wiley, New York, 2001), pp. 57–103.

<sup>11</sup>R. M. A. Azzam and N. M. Bashara, *Ellipsometry and Polarized Light* (North-Holland, Amsterdam, 1977).

<sup>12</sup>C. C. Katsidis, D. I. Siapas, A. K. Robinson, and P. L. F. Hemment, *J. Electrochem. Soc.* **148**, G704 (2001).

<sup>13</sup>C. Q. Sun, X. W. Sun, B. K. Tay, S. P. Lau, H. T. Huang, and S. Li, *J. Phys. D* **34**, 2359 (2001).

<sup>14</sup>V. Ranjan, M. Kapoor, and V. A. Singh, *J. Phys.: Condens. Matter* **14**, 6647 (2002).

<sup>15</sup>C. Q. Sun, H. Q. Gong, P. Hing, and H. T. Ye, *Surf. Rev. Lett.* **6**, 171 (1999).